Journal of Alloys and Compounds, 186 (1992) 111–133
JALCOM 253

Quaternary selenodiphosphates(IV): $M^IM^{III}[P_2Se_6]$, (M^I = Cu, Ag; M^{III} = Cr, Al, Ga, In)

Regine Pfeiff and Rüdiger Kniep*
Eduard-Zintl-Institut, Technische Hochschule Darmstadt, Hochschulstrasse 10,
6100 Darmstadt (Germany)

(Received January 17, 1992)

Abstract

The layered compounds $CuCr[P_2Se_6]$ (m.p. 730 °C, incongruent), $AgCr[P_2Se_6]$ (m.p. 720 °C, incongruent), $AgAl[P_2Se_6]$ (m.p. 588 °C, congruent), $CuIn[P_2Se_6]$ (m.p. 642 °C, incongruent), $AgIn[P_2Se_6]$ (m.p. 673 °C, congruent), α-$AgGa[P_2Se_6]$ (m.p. 450 °C, congruent) and β-$AgGa[P_2Se_6]$ (metastable) were prepared from the elements in evacuated silica tubes (molar ratios M^I:M^{III}:P:Se = 1:1:2:6) by heating up to 750 °C (10 h) followed by quenching/annealing or by cooling from the melt (Bridgman technique).

The crystal structures of $CuIn[P_2Se_6]$, $AgIn[P_2S_6]$ (trigonal, $P\bar{3}1c$; a = 639.2(0), 648.3(1); c = 1333.8(1), 1333.0(4) pm; Z = 2) and β-$AgGa[P_2Se_6]$ (trigonal, $P\bar{3}1c$; a = 637.5(6), c = 1332.0(1) pm; Z = 2) are related to the CdI_2 structure type whereas the crystal structures of $CuCr[P_2Se_6]$, $AgCr[P_2Se_6]$ and $AgAl[P_2Se_6]$ (monoclinic, $C2/m$; a = 619.3(3), 630.5(8), 634.8(5); b = 1072.4(2), 1091.7(3); 1098.9(3); c = 690.9(9), 699.1(1), 702.8(4) pm; β = 107.2(7), 107.7(1), 107.2(1)°; Z = 2) are related to the $CdCl_2$ structure type. α-$AgGa[P_2Se_6]$ (orthorhombic, $Pbca$; a = 1216.9(5), b = 2248.4(6), c = 747.3(2) pm; Z = 4) shows close relationships to the crystal structure of $Ag_4[P_2Se_6]$.

1. Introduction

The first selenodiphosphate(IV), $Fe_2[P_2Se_6]$, was reported by Hahn *et al.* in 1973 [1]. The crystal structure contains Se_6 octahedra with central P–P pairs (corresponds to $[P_2Se_6]^{4-}$ structural units). Today we know a large variety of ternary selenodiphosphates(IV) with M^I (Ag [2]; Tl [3]), M^{II} (Fe [1]; Co, Ni, Mn, Mg, Ca, Cd [4]; Sn, Pb [5]; Hg [6]) and M^{III} (In [7]). The crystal structures of the ternary phases $(M^{II})_2[P_2Se_6]$ are related either to the CdI_2 structure type (for example $Fe_2[P_2Se_6]$, [1]) or to the $CdCl_2$ structure type (for example $Ni_2[P_2Se_6]$, [4]). Selenium atoms are arranged in "close-packed" layers which are stacked with the sequences ...AB... and ...ABC... respectively. M^{II} ions and P_2 pairs occupy the octahedral sites of every second Se double-layer in such a way that the P_2 pairs are surrounded by M^{II} species.

The only ternary M^{III} selenodiphosphate(IV) known up to now was $In_{1.33}\square_{0.67}[P_2Se_6]$ (corresponds to $In_2[P_3Se_9]$) which was found to exist in

---

*Author to whom correspondence should be addressed.

0925-8388/92/$5.00

two different modifications: (i) statistical distribution of In(III) and vacancies on the octahedral sites (trigonal, $R\bar{3}$; $a=637.3(3)$, $c=1986.8(8)$ pm; $Z=3$, [7]); (ii) superstructure $In_{1.33}\Box_{0.67}[P_2Se_6]$ with an ordered distribution of In(III) and vacancies on the octahedral sites (orthorhombic, *Pba*2; $a=1919.7(9)$, $b=1109.0(9)$, $c=2006.7(7)$ pm; $Z=6$, [8]). Investigations of the photoelectrical properties of $In_{1.33}\Box_{0.67}[P_2Se_6]$ showed the ternary phase to be suitable for photovoltaic devices [9].

Together with the knowledge of some new solar-cell materials based on the ternary selenides $CuInSe_2$ and $CuGaSe_2$ [10] we were interested in quaternary selenodiphosphates(IV) containing the cationic components M^I and M^{III} with a molar ratio of 1:1. In other words, the aim was to substitute M^{II} in compounds $(M^{II})_2[P_2Se_6]$ by M^I(Ag, Cu) and M^{III}(Al, Ga, In, Cr) in order to obtain quaternary phases of composition $M^IM^{III}[P_2Se_6]$, [3, 11]. The possibility of substitution of M^{II} cations by M^I(Ag, Cu) and M^{III} (Cr, In, Sc, V) had already been demonstrated for a number of thiodiphosphates(IV) [12–17, 19] as well as for the quaternary selenodiphosphate $AgV[P_2Se_6]$ [18].

2. Experimental details and crystallographic data

Quaternary selenodiphosphates(IV) were prepared from the elements (molar ratios M^I:M^{III}:P:Se = 1:1:2:6) in evacuated silica tubes by heating up to 750 °C (10 h) followed by quenching/annealing (incongruent melting) or by cooling (congruent melting behaviour) from the melt (cooling rate 30 °C h^{-1}). Single-phase products were characterized by differential thermal analysis (DTA) (sealed silica tubes; thermocouples Ni–NiCr; inert reference; heating rate 3 °C min^{-1}) and by X-ray powder diffraction (STOE diffractometer 6.11.1.; position sensitive detector; Cu $K\alpha_1$ radiation; Debye–Scherrer method). In cases of isotypic relations to phases with crystal structures which were already known the structure refinements were carried out by use of the Rietveld full-profile method [20]. Single crystals were investigated on a Philips PW 1100 four-circle diffractometer (Mo $K\alpha$ radiation; graphite monochromator).

Melting points, melting behaviour as well as basic crystallographic data of the compounds under investigation are given in Table 1.

$CuCr[P_2Se_6]$: details concerning the crystal structure determination from X-ray powder data (isotypic relation to $Ni_2[P_2Se_6]$, [4]) and the resulting positional and thermal parameters are summarized in Table 2. X-ray powder patterns (observed and calculated) are given in Fig. 1 and Table 3.

$AgCr[P_2Se_6]$ and $AgAl[P_2Se_6]$: the X-ray powder data are consistent with isotypic relations to $CuCr[P_2Se_6]$ (Fig. 2 and Table 4).

$CuIn[P_2Se_6]$ and $AgIn[P_2Se_6]$: the congruent melting behaviour of $AgIn[P_2Se_6]$ makes it possible to grow single crystals from the melt by use of the Bridgman technique. Large single crystals (1 cm in diameter, 3 cm in length) were obtained in closed (sealed) silica tubes (with seeding capillary

TABLE 1

Quaternary selenodiphosphates(IV), M^IM^{III} [P_2Se_6]: melting points (°C), melting behaviour (i = incongruent; c = congruent), temperature (°C) and time (d) of annealing after quenching the melt to liquid nitrogen, colour (*Eg* (eV)), cleavage and basic crystallographic data ((P) = X-ray powder investigation, (S) = single crystal data)

Compound	Space group	Lattice constants (pm), (°)				
		a	*b*	*c*	*β*	
CuCr[P_2Se_6]	*C*2/*m*	619.3(3)	1072.4(2)	690.9(9)	107.2(7)	*Z*=2 (P)
(730 °C, i; 600 °C, 21 d; dark red (1.13 eV); good cleavage (001))						
AgCr[P_2Se_6]	*C*2/*m*	630.5(8)	1091.7(5)	699.1(1)	107.7(1)	*Z*=2 (P)
(720 °C, i; 550 °C, 21 d; dark red (1.20 eV); good cleavage (001))						
AgAl[P_2Se_6]	*C*2/*m*	634.8(5)	1098.9(3)	702.8(4)	107.2(5)	*Z*=2 (P)
(588 °C, c; 550 °C, 21 d; yellow (2.42 eV); good cleavage (001))						
CuIn[P_2Se_6]	$P\bar{3}1c$	639.2(0)		1333.8(1)		*Z*=2 (P)
(642 °C, i; 500 °C, 14 d; dark red (1.78 eV); perfect cleavage (001))						
AgIn[P_2Se_6]	$P\bar{3}1c$	648.3(1)		1333.0(4)		*Z*=2 (P)
(673 °C, c; 500 °C, 14 d; dark red (1.79 eV); perfect cleavage (001))						
β-AgGa[P_2Se_6]	$P\bar{3}1c$	637.5(6)		1332.0(1)		*Z*=2 (S)
(metastable; dark red (1.91 eV); perfect cleavage (001))						
α-AgGa[P_2Se_6]	*Pbca*	1216.9(5)	2248.4(6)	747.3(2)		*Z*=2 (S)
(450 °C, c; 400 °C, 21 d; yellow-red (2.60 eV); good cleavage (010))						

at the bottom), a maximum temperature of 800 °C and a "dropping-rate" of 4 cm per day. Details concerning the crystal structure determinations (isotypic relation to AgIn[P_2S_6], [12]) and the resulting positional and thermal parameters for AgIn[P_2Se_6] and CuIn[P_2Se_6] are summarized in Tables 5 and 7. X-ray powder patterns (observed and calculated) are given in Tables 6 and 8 and Figs. 3 and 4. The relatively poor *R*(*I*, *hkl*) values of the structure determinations of AgIn[P_2Se_6] and CuIn[P_2Se_6] are presumed to be caused by effects of texture because of the perfect cleavage of the crystals' parallel (001).

AgGa[P_2Se_6]: depending on the special mode of preparation the compound is obtained in two different modifications. α-AgGa[P_2Se_6] is the stable phase under conditions of thermal equilibrium and is prepared by quenching the homogeneous melt followed by annealing at 400 °C for a period of 21 d. By cooling down the melt from 750 °C to room temperature with a rate of 30 °C h^{-1} the metastable β-modification is formed first (Ostwald'sche Stufenregel). β-AgGa[P_2Se_6] can be converted to the stable α-phase by annealing at 350 °C for a period of 14 d. Single crystals were obtained from both modifications. Details concerning the crystal structure determinations and the resulting positional and thermal parameters are given in Tables 9 and 10.

TABLE 2

$CuCr[P_2Se_6]$: data pertaining to the structure determination; positional and thermal parameters; selected interatomic distances (pm) and bond angles (°)

Space group	$C2/m$ (12), monoclinic
Lattice parameters (pm)	$a = 619.3(3)$ $b = 1072.4(2)$ $\beta = 107.2(7)$ $c = 690.9(9)$
Cell volume	690.9 $pm^3 \times 10^6$
Z	2
Calculated density	4.9 g cm^{-3}
Absorption coefficient μ (Cu $K\alpha$)	425.7 cm^{-1}
Diffractometer	STOE, STADI/P Transmission powder diffractometer with position sensitive detector (STOE-PSD)
Radiation	Cu $K\alpha_1$ (Germanium monochromator)
2θ range	$9° < 2\theta < 70°$
Structure solution and refinement	Isotypic relation to $Ni_2[P_2Se_6]$ [4] Rietveld method [20]
Number of measured data points	2027
Number of profile parameters refined	13
Number of positional parameters refined	8
Number of thermal parameters refined	4
R_{WP}; $R(I, h\ k\ l)$	8.6; 10.0

Atom	x	y	z	Occupation	U_{iso} (pm^2)[a]
Cu	0	0.3288(51)	0	0.5	674(95)
Cr	0	0.3288(51)	0	0.5	674(95)
P	0.0538(120)	0	0.1537(56)	1.0	204(138)
Se	0.7402(65)	0	0.2531(29)	1.0	185(87)
Se	0.2486(50)	0.1722(18)	0.2503(17)	1.0	257(53)

Cu/Cr–Se	263.4	2×	Se–Cu/Cr–Se	94.32	1×
	263.7	2×		94.84	2×
	264.1	2×		85.57	2×
				179.63	2×
				85.63	2×
				179.39	1×
				85.52	2×
				94.07	2×
				94.41	1×
P–P	225.6				
P–Se	211.3	1×	P–P–Se	103.76	
	211.5	2×	Se–P–Se	114.32	2×
				114.62	1×
				103.98	2×

[a] U_{iso} is defined as $\exp(-8\pi^2 * U^* \sin^2\theta/\lambda^2)$.

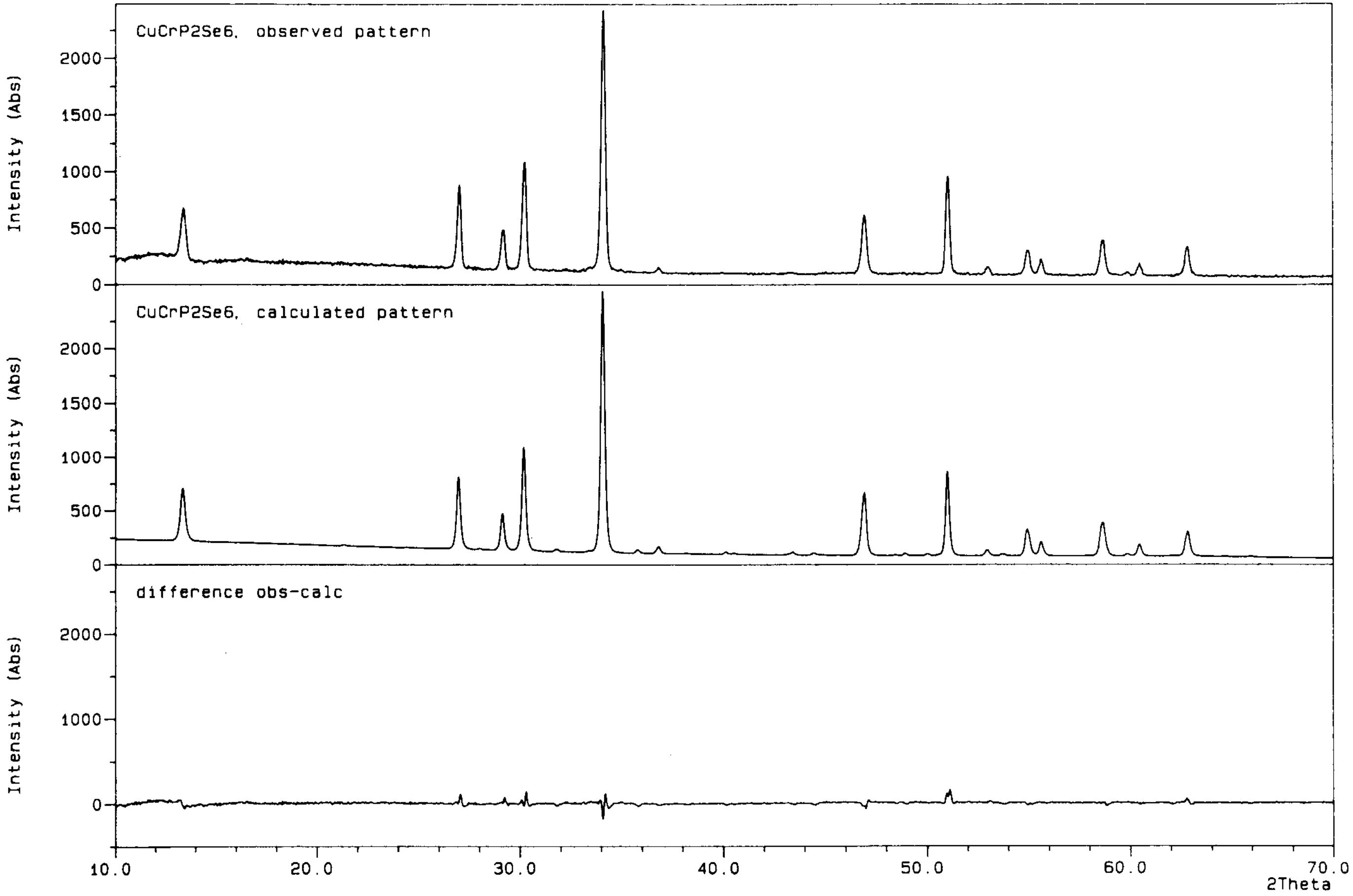

Fig. 1. $CuCr[P_2Se_6]$: observed (top), calculated [20] (middle) and difference (bottom) X-ray powder patterns (Cu $K\alpha_1$).

TABLE 3

CuCr[P_2Se_6]: X-ray powder diffraction data; observed and calculated [20] intensities

$h\,k\,l$	d_{obs} (pm)	FWHM[a]	I_{obs}	I_{calc}	$h\,k\,l$	d_{obs} (pm)	FWHM[a]	I_{obs}	I_{calc}
0 0 1	660.74	0.265	171.88	160.05	3 3 1	157.50	0.211	33.97	35.42
0 2 0	536.22	0.250	10.63	0.62	0 6 2	157.30	0.212	32.74	34.43
$\bar{1}$ 1 1	470.97	0.240	3.15	0.53	$\bar{3}$ 3 3	157.11	0.212	30.56	33.66
0 2 1	416.19	0.230	15.85	3.20	$\bar{2}$ 6 1	154.43	0.215	6.23	5.36
1 1 1	364.28	0.220	6.29	1.94	2 6 0	153.10	0.217	16.38	21.05
0 0 2	330.29	0.212	183.57	177.70	$\bar{4}$ 0 2	152.99	0.217	7.73	10.27
1 3 0	306.21	0.207	50.50	48.97	4 0 0	148.01	0.224	27.94	24.89
$\bar{2}$ 0 1	305.99	0.207	40.71	39.13	$\bar{2}$ 6 2	147.79	0.224	49.00	49.69
2 0 0	296.03	0.204	87.24	84.98	$\bar{3}$ 3 4	138.54	0.242	1.94	0.46
$\bar{1}$ 3 1	295.59	0.204	172.23	166.47	$\bar{1}$ 1 5	136.66	0.246	1.31	0.51
0 2 2	281.28	0.201	2.03	6.66	4 0 1	135.99	0.248	1.69	0.29
0 4 0	268.33	0.198	5.18	2.74	2 4 3	134.74	0.251	2.01	0.64
1 3 1	262.90	0.197	430.49	432.59	$\bar{1}$ 5 4	134.52	0.252	4.11	1.62
$\bar{2}$ 0 2	262.32	0.197	217.05	217.04					
1 1 2	250.71	0.195	0.75	8.28					
2 0 1	244.32	0.194	1.43	2.96					
$\bar{1}$ 3 2	243.91	0.194	5.66	14.33					
$\bar{1}$ 1 3	224.64	0.191	1.60	5.83					
2 2 1	222.33	0.191	1.20	3.88					
0 0 3	220.02	0.191	1.20	0.82					
1 3 2	209.01	0.190	3.56	2.16					
0 4 2	208.27	0.190	5.41	6.37					
0 2 3	203.27	0.191	2.76	5.99					
$\bar{2}$ 4 1	201.74	0.191	5.08	1.00					
2 4 0	198.65	0.191	3.32	0.48					
$\bar{1}$ 5 1	198.51	0.191	3.43	0.51					
$\bar{2}$ 2 3	194.12	0.192	7.09	6.02					
2 0 2	193.81	0.192	49.17	48.48					
$\bar{1}$ 3 3	193.33	0.192	121.24	115.43					
1 5 1	187.64	0.193	4.55	2.41					
1 1 3	186.08	0.194	8.47	5.81					
2 2 2	182.29	0.195	7.44	4.84					
2 4 1	180.59	0.195	1.60	1.06					
$\bar{3}$ 3 1	178.89	0.196	153.96	128.71					
0 6 0	178.88	0.196	76.44	63.85					
3 1 1	172.97	0.196	2.94	1.96					
3 3 0	172.80	0.199	10.24	7.28					
0 6 1	172.67	0.199	5.86	4.06					
$\bar{3}$ 1 3	172.46	0.199	2.28	1.55					
$\bar{3}$ 3 2	170.46	0.199	2.77	1.86					
$\bar{1}$ 1 4	170.50	0.200	1.81	4.06					
0 4 3	170.08	0.201	1.21	2.10					
1 3 3	167.07	0.203	50.61	52.67					
$\bar{2}$ 0 4	166.69	0.203	23.59	25.92					
0 0 4	165.15	0.204	34.34	31.97					
1 5 2	164.84	0.204	2.17	1.99					
$\bar{2}$ 4 3	164.58	0.205	2.59	2.39					
0 2 4	157.71	0.211	1.91	2.14					

[a] Full width at half maximum.

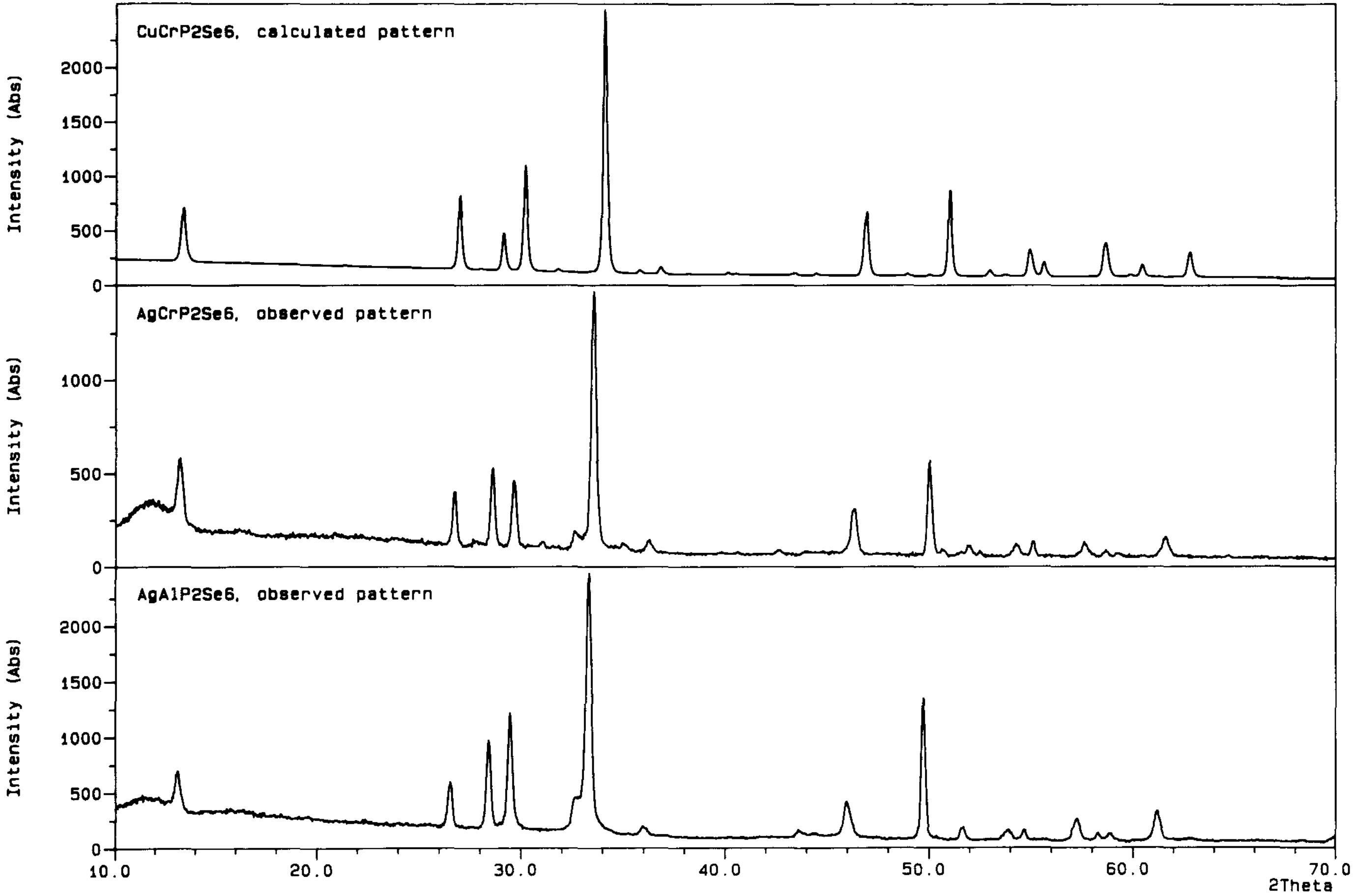

Fig. 2. Comparison of the calculated [20] (top) X-ray powder pattern (Cu Kα_1) of CuCr[P_2Se_6] with the observed X-ray powder patterns (Cu Kα_1) of AgCr[P_2Se_6] (middle) and AgAl[P_2Se_6] (bottom).

TABLE 4

Comparison of the observed X-ray powder data of AgCr[P_2Se_6] and AgAl[P_2Se_6] with the calculated powder data of CuCr[P_2Se_6]

h k l	CuCr[P_2Se_6] (calc.)		AgCr[P_2Se_6] (obs.)		AgAl[P_2Se_6] (obs.)	
	d (pm)	I/I_{max}	*d* (pm)	I/I_{max}	*d* (pm)	I/I_{max}
0 0 1	666.16	36.0	666.15	57.1	671.69	34.8
0 2 0	536.22	2.4	545.87	0.0	549.51	7.4
$\bar{1}$ 1 1	470.97	0.7	478.86	0.0	481.49	1.1
0 2 1	416.19	3.7	422.10	9.6	425.22	0.0
1 1 1	364.28	1.5	367.70	2.4	372.16	0.0
0 0 2	330.08	41.0	332.86	22.8	335.69	27.3
1 3 0	305.19	11.6	311.21	24.0	313.57	10.8
$\bar{2}$ 0 1	305.78	40.7	311.64	6.0	313.25	17.3
2 0 0	295.87	19.6	300.25	9.7	303.24	15.5
$\bar{1}$ 3 1	295.40	38.5	300.84	22.6	302.44	29.7
0 2 2	281.28	1.5	284.44	2.6	286.75	1.3
0 4 0	268.33	0.6	273.20	1.6	274.99	5.9
1 3 1	262.70	100.0	266.27	100.0	268.83	100.0
$\bar{2}$ 0 2	262.11	50.2	267.12	47.4	267.82	45.9
1 1 2	250.71	1.9	252.65	1.6	255.65	0.1
2 0 1	244.32	0.3	246.88	3.0	249.96	0.9
$\bar{1}$ 3 2	243.91	3.3	247.93	4.1	249.13	10.4
1 1 3	224.64	1.3	227.58	0.7	228.60	0.1
2 2 1	222.33	0.2	224.95	0.0	227.53	0.0
0 0 3	220.02	0.3	221.91	0.0	223.78	1.2
1 3 2	209.01	0.8	211.27	0.4	213.43	0.5
0 4 2	208.27	1.4	211.23	1.7	212.79	2.2
0 2 3	203.72	1.3	205.74	1.8	207.44	6.2
$\bar{2}$ 4 1	201.74	1.0	205.47	3.8	206.72	0.1
2 4 0	198.65	0.7	201.94	1.7	203.59	4.3
$\bar{2}$ 2 3	194.12	1.4	197.82	1.6	198.44	0.5
2 0 2	197.66	3.5	195.29	12.9	197.78	13.8
$\bar{1}$ 3 3	193.17	26.7	195.93	23.8	196.93	20.8
1 5 1	187.64	0.4	190.58	1.2	192.13	0.7
1 1 3	186.08	1.3	187.47	1.9	189.57	2.3
2 2 2	182.29	1.1	184.03	0.6	186.25	0.5
2 4 1	180.59	0.4	183.09	0.1	184.89	0.1
$\bar{3}$ 3 1	178.75	29.7	181.99	24.6	183.22	23.6
0 6 0	178.74	14.8	181.95	1.9	183.18	10.7
3 1 1	172.97	0.7	175.02	0.7	177.09	0.9
3 3 0	172.80	1.7	175.51	0.7	177.12	2.4
0 6 1	172.67	0.9	175.66	1.3	176.86	0.4
$\bar{3}$ 1 3	172.46	0.5	175.76	1.9	176.24	1.3
$\bar{3}$ 3 2	170.46	0.6	175.72	3.4	176.54	0.1
$\bar{1}$ 1 4	170.50	0.4	172.49	0.4	173.46	0.1
0 4 3	170.08	0.3	172.18	0.1	173.51	0.3
1 3 3	166.95	12.2	168.54	6.0	170.25	8.3
$\bar{2}$ 0 4	166.67	6.0	169.08	4.0	169.64	2.7
0 0 4	165.02	7.3	166.45	5.5	167.83	4.5

(*continued*)

TABLE 4 (*continued*)

h k l	$CuCr[P_2Se_6]$ (calc.)		$AgCr[P_2Se_6]$ (obs.)		$AgAl[P_2Se_6]$ (obs.)	
	d (pm)	I/I_{max}	*d* (pm)	I/I_{max}	*d* (pm)	I/I_{max}
1 5 2	164.84	0.5	167.07	0.5	168.55	0.1
$\bar{2}$ 4 3	164.58	0.6	167.44	0.1	168.13	0.1
0 2 4	157.71	0.4	159.19	0.4	160.51	0.2
3 3 1	157.37	8.2	159.41	2.3	161.14	5.4
0 6 2	157.17	8.0	159.66	3.6	160.78	4.8
$\bar{3}$ 3 3	157.00	8.0	159.96	4.3	160.50	3.4
$\bar{2}$ 6 1	154.43	1.2	157.25	0.5	158.26	1.2
2 6 0	152.99	5.0	155.61	2.0	156.79	3.3
$\bar{4}$ 0 2	152.99	2.3	155.93	1.2	156.74	1.1
4 0 0	147.90	5.7	150.10	4.3	151.58	5.0
$\bar{2}$ 6 2	147.84	11.5	150.38	8.0	151.20	2.2
$\bar{3}$ 3 4	138.54	0.4	141.00	0.1	141.87	0.7
$\bar{1}$ 1 5	136.66	0.3	138.16	0.5	139.36	0.4
4 0 1	135.99	0.4	137.65	0.0	139.50	0.3
2 4 3	134.74	0.5	136.09	0.3	137.84	0.4
$\bar{1}$ 5 4	134.52	0.9	136.40	0.8	137.59	0.1

Without exception, the crystals of metastable β-$AgGa[P_2Se_6]$ were of very poor quality because of their perfect cleavage parallel (001) and their extreme sensitivity against mechanical strain (preferably bent crystals). The structure determination was started with the atomic positional parameters of the isotypic phase $AgIn[P_2S_6]$, [12]. Observed and calculated X-ray powder data of β-$AgGa[P_2Se_6]$ are given in Table 11. Again, the relatively poor consistency of the calculated and observed intensities is presumed to be caused by effects of texture because of the perfect cleavage of the crystals' parallel (001).

3. Crystal structures, results and discussion

The crystal structures of the isotypic phases $CuIn[P_2Se_6]$, $AgIn[P_2Se_6]$ and β-$AgGa[P_2Se_6]$ are closely related to the CdI_2-type structure. The selenium atoms form a h.c.p. arrangement with the layer sequence ...AB... running along the [001] direction (Fig. 5). The octahedral sites of every second selenium double-layer are occupied by M^I, M^{III} and P_2 pairs in such a way that the P_2 pairs within the (001) planes are alternately surrounded by M^I and M^{III} species (ordered distribution). The occupied octahedral layers turn with the sequence ...ab... along the [001] direction.

The isotypic phases $CuCr[P_2Se_6]$, $AgCr[P_2Se_6]$ and $AgAl[P_2Se_6]$ show close relations to the $CdCl_2$ type structure. The selenium atoms form a c.c.p. arrangement with the layer sequence ...ABC... running along the [001] direction. M^I, M^{III} and P_2 pairs occupy the octahedral sites of every second

TABLE 5

$AgIn[P_2Se_6]$: data pertaining to the structure determination; positional and thermal parameters; selected interatomic distances (pm) and bond angles (°)

Space group	$P\bar{3}1c$ (163), trigonal
Lattice parameters (pm)	$a = 648.3(1)$ $c = 1333.0(4)$
Cell volume	485.2 $pm^3 \times 10^6$
Z	2
Calculated density	10.4 g cm^{-3}
Absorption coefficient μ (Cu Kα)	1220.0 cm^{-1}
Diffractometer	STOE, STADI/P Transmission powder diffractometer with position sensitive detector (STOE-PSD)
Radiation	Cu $K\alpha_1$ (Germanium monochromator)
2θ range	$10° < 2\theta < 100°$
Structure solution and refinement	Isotypic relation to $AgIn[P_2S_6]$ [12] Rietveld method [20]
Number of measured data points	1705
Number of profile parameters refined	12
Number of positional parameters refined	9
Number of thermal parameters refined	4
R_{WP}; $R(I, h\ k\ l)$	7.9; 17.1

Atom	x	y	z	Occupation	U_{iso} (pm^2)[a]
Ag	0.6667	0.3333	0.25	1.0	752(115)
In	0	0	0.25	1.0	290(72)
P	0.3333	0.6667	0.1618(29)	1.0	5(128)
Se	0.3291(38)	0.3474(36)	0.1178(7)	1.0	281(34)

Ag–Se	284.7	6×	Se–Ag–Se	85.7	6×
				92.0	3×
				96.5	3×
				176.7	3×
In–Se	281.6	6×	Se–In–Se	85.0	6×
				92.2	3×
				97.9	3×
				175.7	3×
P–P	234.9				
P–Se	213.5	3×	P–P–Se	103.7	3×
			Se–P–Se	59.5	3×
				86.5	3×
				87.7	3×
				112.7	3×
				140.9	3×

---

[a] U_{iso} is defined as $\exp(-8\pi^2 * U * \sin^2\theta/\lambda^2)$.

TABLE 6

AgIn[P_2Se_6]: X-ray powder diffraction data; observed and calculated [20] intensities

$h\,k\,l$	d_{obs} (pm)	FWHM[a]	I_{obs}	I_{calc}	$h\,k\,l$	d_{obs} (pm)	FWHM[a]	I_{obs}	I_{calc}
0 0 2	666.65	0.294	217.50	220.63	3 0 6	143.13	0.424	17.13	14.22
1 0 0	561.49	0.298	6.54	3.16	2 1 7	141.73	0.427	2.35	2.39
1 0 1	517.50	0.300	1.77	9.46	2 1 $\bar{7}$	141.73	0.427	6.50	6.60
1 0 2	429.56	0.306	28.81	23.50	3 1 $\bar{4}$	141.08	0.428	3.49	3.90
1 0 3	348.48	0.315	103.41	80.59	3 1 4	141.08	0.428	3.75	4.19
0 0 4	333.35	0.318	94.04	66.68	4 0 1	139.59	0.431	3.34	1.41
1 1 0	324.19	0.319	27.33	8.76	4 0 2	137.35	0.435	2.64	1.06
1 1 $\bar{2}$	291.54	0.326	848.73	776.72	3 1 5	134.47	0.441	11.65	9.32
1 1 2	291.54	0.326	31.22	28.57	3 1 $\bar{5}$	134.47	0.441	2.98	2.39
1 0 4	286.61	0.327	40.25	30.70	4 0 3	133.84	0.443	6.38	4.74
2 0 0	280.73	0.329	10.33	3.42	2 1 $\bar{8}$	131.06	0.449	1.91	1.70
2 0 1	274.77	0.330	32.12	14.82	2 1 8	131.06	0.449	2.62	2.33
1 0 5	240.87	0.342	16.24	45.69	2 2 6	130.94	0.449	11.47	10.31
2 0 3	237.37	0.343	3.46	4.27	2 2 $\bar{6}$	130.94	0.449	17.04	15.32
1 1 $\bar{4}$	232.36	0.345	77.15	91.52	4 0 4	129.36	0.453	3.87	4.08
1 1 4	232.36	0.345	159.09	188.71	3 2 $\bar{1}$	128.21	0.456	2.46	1.90
0 0 6	222.18	0.350	2.92	17.62	3 1 $\bar{6}$	127.51	0.458	2.50	2.00
2 0 4	214.74	0.354	1.95	8.19	3 1 6	127.51	0.458	3.68	2.94
2 1 1	209.56	0.357	4.70	9.91	3 2 $\bar{2}$	126.46	0.461	3.11	1.48
1 0 6	206.60	0.358	2.40	12.53	3 0 8	124.45	0.466	48.73	48.22
2 0 5	193.33	0.367	2.56	10.27	4 0 5	124.20	0.467	4.80	4.91
2 1 3	191.52	0.368	10.17	10.75	1 1 $\overline{10}$	123.28	0.470	39.96	34.55
3 0 0	187.18	0.372	233.06	210.87	2 1 9	121.45	0.475	2.30	1.36
1 1 6	183.29	0.375	72.10	76.47	4 1 $\bar{2}$	120.50	0.478	53.29	46.72
1 1 $\bar{6}$	183.29	0.375	34.33	36.41	4 1 2	120.50	0.478	2.81	2.47
1 0 7	180.34	0.377	7.75	6.41	3 2 4	120.14	0.479	1.47	1.16
3 0 2	180.20	0.378	30.82	26.35	3 2 $\bar{4}$	120.14	0.479	1.13	0.89
2 1 4	179.02	0.379	4.50	4.86	4 1 $\bar{4}$	114.99	0.497	6.65	6.88
2 1 $\bar{4}$	179.02	0.379	5.43	5.86	4 1 4	114.99	0.497	15.33	15.85
2 0 6	174.22	0.383	1.34	8.20	4 1 $\bar{6}$	107.28	0.531	8.66	9.65
0 0 8	166.65	0.391	34.08	31.91	4 1 6	107.28	0.531	9.41	10.49
2 1 $\bar{5}$	166.04	0.392	14.97	16.41	3 2 7	106.69	0.534	3.87	3.73
3 0 4	163.19	0.395	37.12	40.16	3 2 $\bar{7}$	106.69	0.534	1.84	1.77
1 0 8	159.76	0.399	5.81	2.80	3 3 $\bar{2}$	106.66	0.534	1.14	1.10
2 0 7	157.59	0.402	12.34	10.67	3 3 2	106.66	0.534	1.24	1.19
2 2 2	157.49	0.402	91.42	81.11	4 2 $\bar{1}$	105.77	0.539	1.87	1.39
2 2 $\bar{2}$	157.49	0.402	4.26	3.78	1 1 $\overline{12}$	105.08	0.542	2.61	2.31
3 1 1	154.68	0.406	3.65	2.49	1 1 12	105.08	0.542	17.81	15.74
2 1 6	153.45	0.408	3.76	3.47	4 2 3	103.20	0.553	1.27	1.25
2 1 $\bar{6}$	153.45	0.408	8.00	7.38	2 2 10	103.00	0.554	14.52	15.50
3 1 2	151.65	0.410	3.96	2.03	3 3 4	102.78	0.555	3.35	3.31
1 1 8	148.20	0.416	8.42	5.64	3 3 $\bar{4}$	102.78	0.555	3.32	3.28
1 1 $\bar{8}$	148.20	0.416	2.11	1.41	3 2 $\bar{8}$	101.91	0.561	1.71	1.31
3 1 $\bar{3}$	146.96	0.418	10.61	7.64	3 2 8	101.91	0.561	1.20	0.91
3 1 3	146.96	0.418	2.95	2.13					
2 2 4	145.76	0.420	15.27	12.54					
2 2 $\bar{4}$	145.76	0.420	33.06	27.14					
2 0 8	143.30	0.424	3.65	3.04					

[a] Full width at half maximum.

TABLE 7

$CuIn[P_2Se_6]$: data pertaining to the structure determination; positional and thermal parameters; selected interatomic distances (pm) and bond angles (°)

Space group	$P\bar{3}1c$ (163), trigonal
Lattice parameters (pm)	$a = 639.2(0)$ $c = 1333.8(1)$
Cell volume	472.0 $pm^3 \times 10^6$
Z	2
Calculated density	10.0 g cm^{-3}
Absorption coefficient μ (Cu Kα)	980.8 cm^{-1}
Diffractometer	STOE, STADI/P Transmission powder diffractometer with position sensitive detector (STOE-PSD)
Radiation	Cu Kα_1 (Germanium monochromator)
2θ range	$10° < 2\theta < 100°$
Structure solution and refinement	Isotypic relation to $AgIn[P_2S_6]$ [12] Rietveld method [20]
Number of measured data points	1705
Number of profile parameters refined	12
Number of positional parameters refined	9
Number of thermal parameters refined	4
R_{WP}; $R(I, h\ k\ l)$	9.4; 19.6

Atom	x	y	z	Occupation	U_{iso} (pm^2)[a]
Cu	0.6667	0.3333	0.25	1.0	3781(617)
In	0	0	0.25	1.0	154(36)
P	0.3333	0.6667	0.1655(24)	1.0	5(96)
Se	0.3306(24)	0.3401(25)	0.1201(7)	1.0	141(19)

Cu–Se	277.7	6×	Se–Cu–Se	85.2	6×
				93.7	3×
				95.9	3×
				178.4	3×
In–Se	275.7	6×	Se–In–Se	84.7	6×
				93.8	3×
				96.8	3×
				177.8	3×
P–P	225.3				
P–Se	216.5	3×	P–P–Se	106.2	3×
			Se–P–Se	61.2	3×
				86.4	3×
				87.2	3×
				112.5	3×
				142.3	3×

[a] U_{iso} is defined as $\exp(-8\pi^2 {*} U {*} \sin^2\theta/\lambda^2)$.

TABLE 8

CuIn[P_2Se_6]: X-ray powder diffraction data; observed and calculated [20] intensities

h k l	d_{obs} (pm)	FWHM[a]	I_{obs}	I_{calc}	*h k l*	d_{obs} (pm)	FWHM[a]	I_{obs}	I_{calc}
0 0 2	660.90	0.230	293.21	328.17	2 1 7	140.88	0.267	1.14	1.16
1 0 0	553.64	0.232	6.49	58.33	2 1 $\bar{7}$	140.88	0.267	4.49	4.57
1 0 2	425.97	0.235	172.64	138.46	3 1 $\bar{4}$	139.47	0.268	16.13	14.28
1 0 3	346.65	0.238	62.58	23.76	3 1 4	139.47	0.268	16.50	14.60
0 0 4	333.45	0.238	360.61	238.83	4 0 2	135.52	0.270	7.01	6.27
1 1 0	319.63	0.239	20.24	1.90	2 1 $\bar{8}$	130.39	0.272	8.89	9.64
1 1 $\bar{2}$	288.23	0.241	1492.83	1388.04	2 1 8	130.39	0.272	9.53	10.33
1 1 2	288.23	0.241	189.27	175.98	2 2 6	129.76	0.273	41.23	41.20
1 0 4	285.64	0.241	114.71	121.16	2 2 $\bar{6}$	129.76	0.273	41.67	41.64
2 0 0	276.80	0.242	36.71	21.72	1 0 10	129.67	0.273	5.18	5.00
2 0 1	271.03	0.242	7.16	0.64	4 0 4	127.83	0.274	15.87	11.70
2 0 2	255.66	0.244	27.67	46.06	3 2 0	127.01	0.274	5.45	4.04
1 1 $\bar{4}$	230.75	0.247	122.72	160.73	3 2 1	126.43	0.275	1.54	1.19
1 1 4	230.75	0.247	223.73	293.03	3 1 $\bar{6}$	126.33	0.275	13.42	10.14
2 0 4	212.98	0.249	27.51	47.52	3 1 6	126.33	0.275	15.93	12.03
2 1 0	209.25	0.249	9.02	20.16	3 2 2	124.76	0.276	5.04	3.32
2 1 $\bar{1}$	206.72	0.250	6.30	10.40	3 2 $\bar{2}$	124.76	0.276	8.44	5.56
1 0 6	206.29	0.250	42.12	59.41	3 0 8	123.71	0.276	121.63	126.50
2 1 $\bar{2}$	199.65	0.251	15.76	19.40	1 1 $\overline{10}$	123.09	0.277	82.63	82.49
2 1 2	199.65	0.251	23.42	28.82	1 1 10	123.09	0.277	5.41	5.41
2 0 5	192.08	0.252	4.18	4.04	4 0 5	122.85	0.277	3.77	3.64
2 1 3	189.32	0.253	2.78	1.43	3 3 3	122.12	0.278	2.64	1.49
3 0 0	184.54	0.254	530.33	417.90	2 0 10	120.16	0.279	3.51	3.47
1 1 6	182.50	0.254	130.37	159.03	4 1 $\bar{2}$	118.87	0.280	157.25	122.43
1 1 $\bar{6}$	182.50	0.254	111.54	136.06	4 1 2	118.87	0.280	26.13	20.35
1 0 7	180.17	0.255	5.81	3.30	3 2 4	118.69	0.280	8.36	6.12
3 0 2	177.85	0.255	44.70	28.46	3 2 $\bar{4}$	118.69	0.280	7.96	5.83
2 1 4	177.24	0.256	34.58	27.87	4 0 6	117.49	0.281	11.04	8.43
2 1 $\bar{4}$	177.24	0.256	35.86	28.90	2 2 $\bar{8}$	115.37	0.283	3.62	10.10
2 0 6	173.33	0.257	41.95	35.16	4 1 $\bar{4}$	113.58	0.284	24.75	21.11
0 0 8	166.73	0.258	63.47	67.34	4 1 4	113.58	0.284	47.34	40.39
2 1 $\bar{5}$	164.64	0.259	8.41	8.47	3 1 8	112.94	0.285	4.19	4.91
3 0 4	161.46	0.260	168.52	170.30	3 1 $\bar{8}$	112.94	0.285	4.41	5.17
1 0 8	159.64	0.260	19.23	18.95	3 2 6	110.28	0.287	1.72	8.58
2 0 7	156.95	0.261	8.94	6.32	3 3 0	106.54	0.291	75.97	56.81
2 2 2	155.42	0.262	206.30	169.69	4 0 8	106.49	0.291	5.08	3.69
2 2 $\bar{2}$	155.42	0.262	34.41	28.31	4 1 $\bar{6}$	106.15	0.291	51.88	41.93
3 1 0	153.55	0.262	6.51	5.49	4 1 6	106.15	0.191	47.90	38.71
3 1 $\bar{1}$	152.54	0.263	2.00	2.25	3 2 7	105.68	0.292	4.12	3.75
3 1 1	152.54	0.263	8.41	9.50	3 3 $\bar{2}$	105.21	0.292	2.39	2.09
2 1 6	152.36	0.263	16.75	19.66	3 3 2	105.21	0.292	2.42	2.12
2 1 $\bar{6}$	152.36	0.263	21.52	25.26	5 0 4	105.08	0.292	4.62	4.00
3 1 $\bar{2}$	149.63	0.264	10.81	10.35	1 1 12	104.98	0.293	48.63	40.09
3 1 2	149.63	0.264	8.30	7.95	1 1 $\overline{12}$	104.98	0.293	11.25	9.27
1 1 8	147.82	0.264	27.31	24.60	2 2 $\overline{10}$	102.40	0.296	3.08	2.71
3 1 $\bar{3}$	145.13	0.266	4.49	2.18	2 2 10	102.40	0.296	51.14	44.99
2 2 4	144.12	0.266	33.13	27.33	3 3 4	101.49	0.297	16.57	16.97
2 2 $\bar{4}$	144.12	0.266	62.51	51.57	3 3 $\bar{4}$	101.49	0.297	16.56	16.96
2 0 8	142.82	0.266	15.22	14.66	3 2 8	101.03	0.297	6.18	4.71
3 0 6	141.99	0.267	15.22	13.25	3 2 $\bar{8}$	101.03	0.297	6.72	5.12

[a] Full width at half maximum.

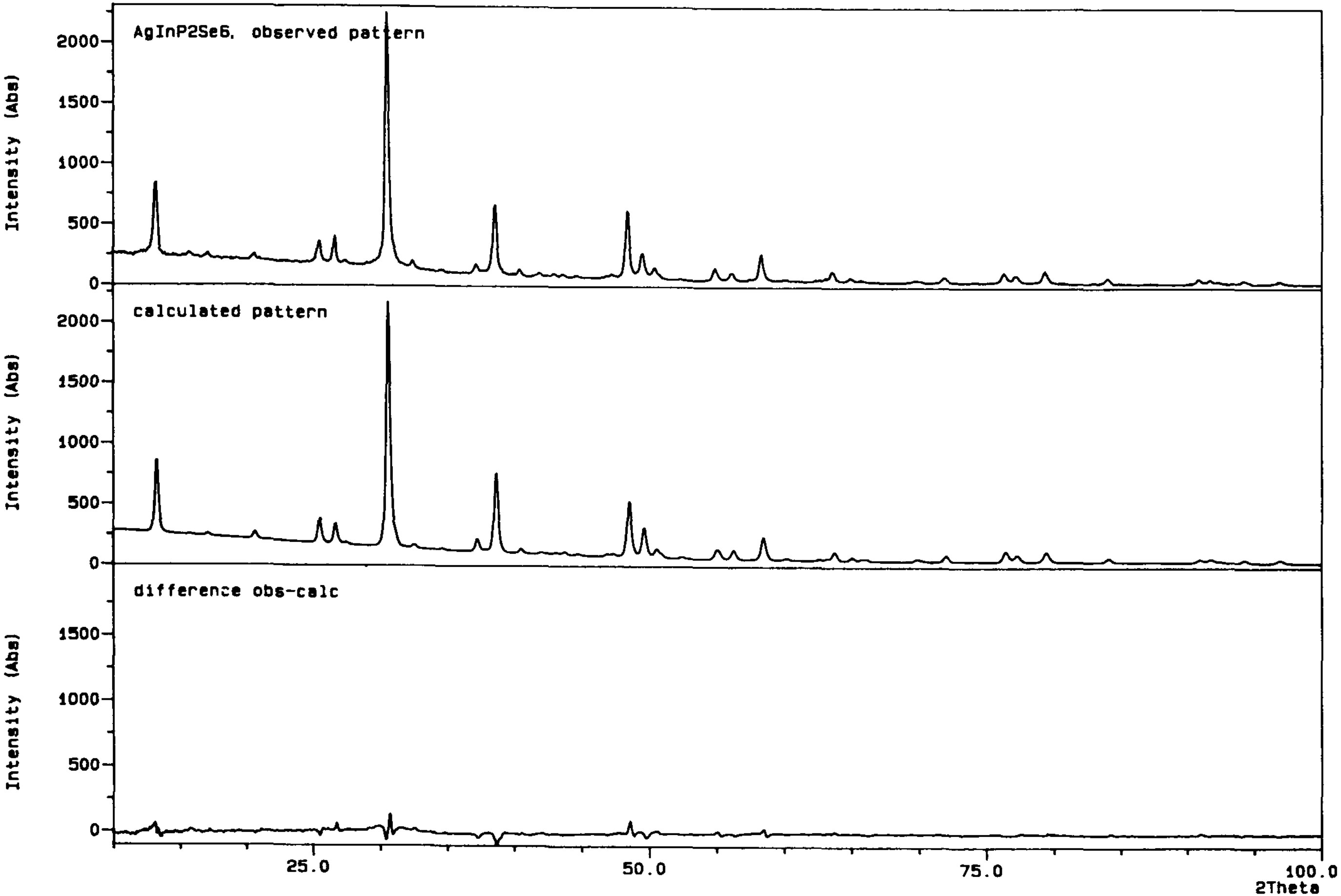

Fig. 3. AgIn[P_2Se_6]: observed (top), calculated [20] (middle) and difference (bottom) X-ray powder patterns (Cu Kα_1).

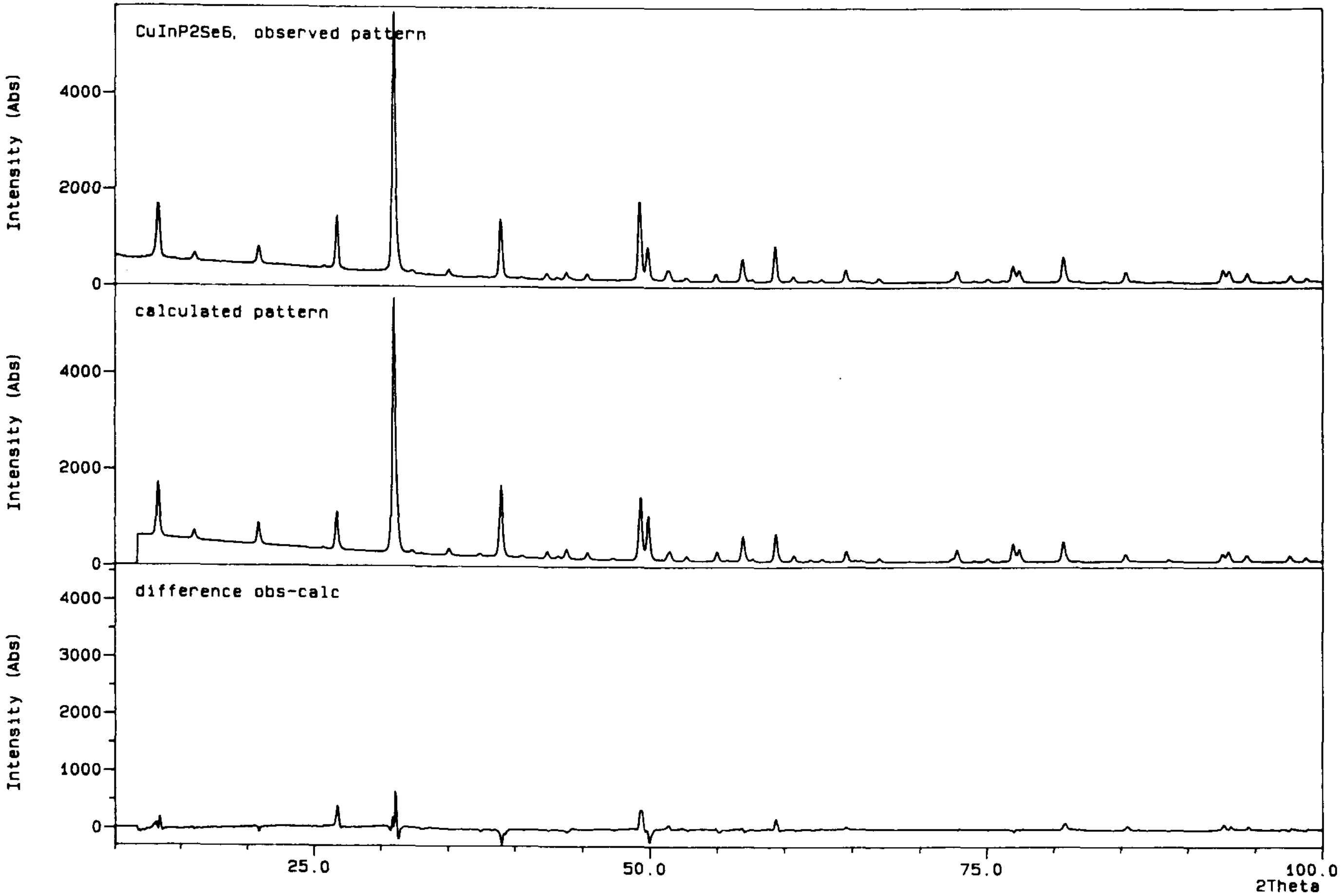

Fig. 4. $CuIn[P_2Se_6]$: observed (top), calculated [20] (middle) and difference (bottom) X-ray powder patterns (Cu $K\alpha_1$).

TABLE 9

Crystallographic data, positional parameters and the interatomic distances (pm) and angles (°) of α-AgGa[P_2Se_6]

Crystallographic data

Space group	*Pbca* (61)
Lattice parameters (pm)	$a = 1216.9(5)$ $b = 2248.4(6)$ $c = 747.3(2)$
Cell volume	2044.67 $pm^3 \times 10^6$
Z	4
Calculated density	2.32 g cm^{-3}

Data collection

Diffractometer	Four-circle Philips PW 1100 diffractometer,
Radiation	Mo Kα, graphite monochromator
Scan mode	$\theta/2\theta$
Number of measured reflections ($5° \leqslant 2\theta \leqslant 90°$)	1541
Number of observed reflections ($I \geqslant 2\sigma(I)$)	855
Number of refined parameters	91
Absorption coefficient μ(Mo Kα)	92.7 cm^{-1}
Absorption correction	DIFABS [21]
Structure solution and refinement	SHELX-86 [22]
Final *R* (aniso)	0.0622

Positional and thermal parameters[a, b]

Atom	x	y	z	U_{eq} (pm^2)[a]
Ag	0.3997(4)	0.9839(2)	0.1593(6)	519(17)
Ga	0.3652(3)	0.1583(2)	0.2708(6)	187(22)
P	0.0995(7)	0.1567(4)	0.4557(15)	121(45)
P	0.6269(9)	0.0877(4)	0.2586(15)	184(52)
Se	0.2341(3)	0.1329(2)	0.0398(5)	200(19)
Se	0.5063(3)	0.2274(2)	0.1885(6)	188(19)
Se	0.3040(3)	0.9933(2)	0.8483(6)	226(21)
Se	0.2636(3)	0.1918(2)	0.5293(6)	249(20)
Se	0.4906(3)	0.8797(2)	0.1756(5)	225(20)
Se	0.4636(3)	0.0695(2)	0.3754(5)	163(19)

Atom	U_{11}	U_{22}	U_{33}	U_{12}	U_{13}	U_{23}
Ag	791(31)	332(21)	435(24)	174(22)	−279(25)	179(19)
Ga	116(20)	232(22)	212(24)	−37(19)	−24(19)	23(20)
P	87(43)	61(39)	215(52)	−4(38)	10(42)	26(41)
P	266(56)	110(48)	176(52)	−21(46)	−51(48)	125(45)
Se	129(17)	288(21)	183(18)	−31(19)	45(18)	60(19)
Se	186(19)	143(17)	234(20)	15(16)	47(19)	73(17)
Se	214(19)	216(21)	249(22)	63(17)	−58(19)	−69(19)

(*continued*)

TABLE 9 (*continued*)

Atom	U_{11}	U_{22}	U_{33}	U_{12}	U_{13}	U_{23}
Se	154(18)	363(22)	230(20)	−12(19)	8(20)	−125(21)
Se	228(20)	232(21)	216(19)	−10(18)	−51(19)	−56(20)
Se	168(18)	152(19)	168(19)	−50(15)	−7(17)	25(17)

Interatomic distances and angles

Ag–Se(2)	262.8(5)	Se(6)–Ag–Se(4)	107.7(2)
Ag–Se(4)	260.8(6)	Se(6)–Ag–Se(2)	120.4(2)
Ag–Se(4*)	290.0(4)	Se(6)–Ag–Se(4*)	120.1(2)
Ag–Se(6)	259.5(6)	Se(4)–Ag–Se(2)	128.3(2)
		Se(4)–Ag–Se(4*)	92.2(2)
		Se(2)–Ag–Se(4*)	79.8(1)
Ga–Se(1)	241.8(6)	Se(3)–Ga–Se(1)	116.2(2)
Ga–Se(2)	245.6(6)	Se(3)–Ga–Se(2)	105.0(2)
Ga–Se(3)	239.6(6)	Se(3)–Ga–Se(5)	111.7(2)
Ga–Se(5)	241.5(6)	Se(1)–Ga–Se(2)	110.9(2)
		Se(1)–Ga–Se(5)	107.8(2)
		Se(5)–Ga–Se(2)	104.4(2)
P(1)–P(2)	225.9(8)		
P(1)–Se(6)	213.8(5)	P(2)–P(1)–Se(6)	111.4(2)
P(1)–Se(5)	221.7(6)	P(2)–P(1)–Se(5)	105.9(2)
P(1)–Se(3)	223.0(4)	P(2)–P(1)–Se(3)	103.2(2)
		Se(6)–P(1)–Se(5)	114.0(2)
		Se(6)–P(1)–Se(3)	112.5(3)
		Se(5)–P(1)–Se(3)	108.9(2)
P(2)–Se(4)	214.8(5)	P(1)–P(2)–Se(4)	112.3(2)
P(2)–Se(1)	221.3(5)	P(1)–P(2)–Se(1)	105.0(2)
P(2)–Se(2)	224.4(2)	P(1)–P(2)–Se(2)	104.8(2)
		Se(4)–P(1)–Se(1)	115.2(2)
		Se(4)–P(1)–Se(2)	109.2(2)
		Se(1)–P(1)–Se(2)	109.6(3)

[a] U_{eq} is defined as $\frac{1}{3}(\Sigma_i \Sigma_j U_{ij} a_i^* a_j^* a_{ij})$.

[b] U_{ij} is defined as $\exp[-2\pi^2(U_{11}h^2a^{*2} + \ldots + 2U_{12}hka^*b^* + \ldots)]$.

selenium double-layer (Fig. 6). The P_2 pairs within the (010) planes are in a random surrounding by M^I and M^{III} species. The occupied octahedral layers run with the sequence ...abc... along the [010] direction.

The crystal structure of α-AgGa[P_2Se_6] contains [P_2Se_6] octahedra which share common edges with [$GaSe_4$] tetrahedra, thereby giving polyhedral chains running within (010) planes parallel to the [100] direction. Along [010] adjacent chains (planes) are interconnected by sharing common edges and common apices with [$AgSe_4$] tetrahedra. The resulting layer structure is shown in Fig. 7. The structure is related to the crystal structure of Ag_4[P_2Se_6] [2] which also contains the metal atoms in tetrahedral coordination and which shows similar principles of polyhedral condensation ([P_2Se_6] octahedra sharing common edges and apices with [$AgSe_4$] tetrahedra). As distinguished

TABLE 10

Crystallographic data, positional parameters and interatomic distances (pm) and angles (°) of β-$AgGa[P_2Se_6]$

Crystallographic data	
Space group	$P\bar{3}1c$ (163)
Lattice parameters (pm)	$a = 637.5(6)$ $c = 1332.0(12)$
Cell volume	468.81 $pm^3 \times 10^6$
Z	2
Calculated density	5.05 g cm^{-3}

Data collection

Diffractometer	Four-circle Philips PW 1100 diffractometer,
Radiation	Mo $K\alpha$, graphite monochromator
Scan mode	$\theta/2\theta$
Number of measured reflections ($5° \leqslant 2\theta \leqslant 90°$)	1537
Number of observed reflections ($I \geqslant 2\sigma(I)$)	392
Number of refined parameters	16
Absorption coefficient μ(Mo $K\alpha$)	92.7 cm^{-1}
Absorption correction	DIFABS [21]
Structure solution and refinement	SHELX-86 [22]
Final R (aniso)	0.245

Atom parameters and temperature factors

Atom	x/a	y/b	z/c	U_{eq} (pm^2)[a]
Ag	2/3	1/3	1/4	521(84)
Ga	0	0	1/4	275(70)
Se	0.3015(9)	0.3218(1)	0.1214(5)	232(22)
P	1/3	2/3	0.1718(24)	242(57)

Atom	U_{11}	U_{22}	U_{33}	U_{12}	U_{13}	U_{23}
Ag	196(39)	196(39)	1171	98(19)	0(0)	0(0)
Ga	106(41)	106(41)	614	53(21)	0(0)	0(0)
Se	1(2)		536(36)	−6(8)	22(23)	−5(6)

Interatomic distances and angles

Ag–Se	286.2(6)	6×	Se–Ag–Se	87.9(9)	6×
				93.9(2)	3×
				90.4(2)	3×
				177.5(0)	3×
Ga–Se	262.6(6)	6×	Se–Ga–Se	101.3(3)	3×
				94.8(3)	3×
				82.0(2)	6×
				175.0(3)	3×
P–P	206.7(6)				
P–Se	221.1(11)	3×	P–P–Se	107.9(0)	3×
			Se–P–Se	111.0(7)	3×

[a] U_{eq} is defined as $\frac{1}{3}(\Sigma_i \Sigma_j a_i^* a_j^* a_{ij})$.

TABLE 11

β-AgGa[P_2Se_6] comparison of the observed and calculated X-ray powder data

h k l	d_{calc} (pm)	$I/I_{max\ calc}$	d_{obs} (pm)	$I/I_{max\ obs}$
0 0 2	666.00	26.5	665.56	14.7
1 0 3	345.99	10.1	343.66	45.0
0 0 4	333.00	12.1	332.18	41.7
1 1 $\bar{2}$	287.51	100.0	286.63	100.0
2 0 1	270.30	3.5	268.49	7.2
1 0 5	239.92	6.5	238.19	4.8
1 1 4	230.26	35.8	228.68	20.1
3 0 0	184.03	23.6	183.20	24.1
1 1 6	182.17	16.0	181.63	8.2
3 0 2	177.38	3.8	176.74	5.2
0 0 8	166.50	4.2	166.24	8.1
2 1 5	164.27	2.7	163.96	8.1
3 0 4	161.07	3.9	160.54	5.5
2 2 2	154.99	9.2	154.31	11.1
2 2 4	143.75	5.0	143.32	8.1
2 2 6	129.46	3.0	129.12	6.3
3 0 8	123.46	5.1	123.00	7.2

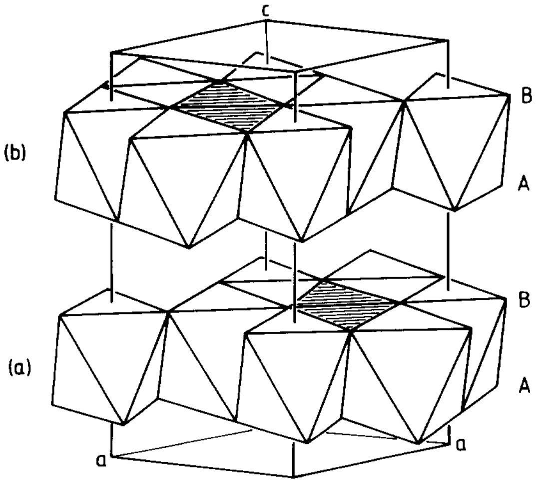

Fig. 5. Crystal structure of the isotypic phases CuIn[P_2Se_6], AgIn[P_2Se_6] and β-AgGa[P_2Se_6] in polyhedral representation. Selenium atoms occupy the apices of the octahedra. The shaded octahedra contain the P_2 pairs; M^I and M^{III} are situated inside the unshaded octahedra (ordered distribution).

from α-AgGa[P_2Se_6] (layer structure) the crystal structure of Ag_4[P_2Se_6] [2] is based on a three-dimensional framework.

The bond lengths In–Se (275.7 pm and 281.6 pm) and Ga–Se (262.6 pm) in the crystal structures of CuIn[P_2Se_6], AgIn[P_2Se_6] and β-AgGa[P_2Se_6] correspond very well with the sum of the ionic radii (M^{III} in octahedral

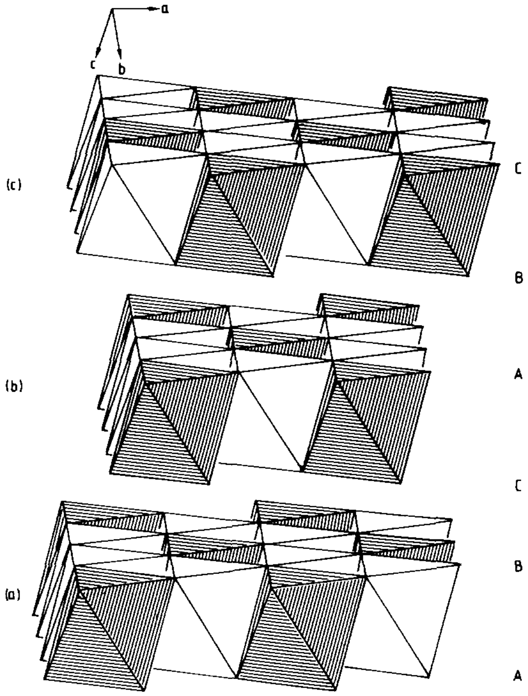

Fig. 6. Crystal structure of the isotypic phases CuCr[P_2Se_6], AgCr[P_2Se_6] and AgAl[P_2Se_6] in polyhedral representation. Selenium atoms occupy the apices of the octahedra. The shaded octahedra contain the P_2 pairs; M^I and M^{III} are situated inside the unshaded octahedra (random distribution).

coordination) given by Pauling [23] (279.0 pm, 260.0 pm). The distances Cu/Cr–Se (263.4–264.1 pm) in the crystal structure of CuCr[P_2Se_6] are consistent with an average value of 272.0 pm, calculated from the sum of the ionic radii (Cr^{III}–Se: 267.0 pm [23]) and the observed bond length Cu–Se (277.7 pm) in the crystal structure of CuIn[P_2Se_6]. The distances Ag–Se in the octahedral layer structures of AgIn[P_2Se_6] and β-AgGa[P_2Se_6] (284.7 pm and 286.2 pm) are much smaller than calculated from the data given by Pauling ([23]; 324.0 pm) but they are in good agreement with the respective value in the crystal structure of AgV[P_2Se_6] ([18]; 287.0 pm).

The bond lengths P–Se in the crystal structures of CuIn[P_2Se_6], AgIn[P_2Se_6] and CuCr[P_2Se_6] are nearly constant (216.5 pm, 213.5 pm and 211.3–211.5 pm) and do not directly depend on the size (average size) of the metal ions which participate in the formation of the compounds. The PSe_3 groups in this way appear as rigid entities, an observation already made by Brec *et al.* [24] for the respective thio compounds. On the other hand, the P–P distances within the [P_2Se_6] groups include the possibility of variation in order to accommodate the metal sizes (P–P: 225.3 pm (CuIn[P_2Se_6]), 225.6 pm (CuCr[P_2Se_6]) and 234.9 pm (AgIn[P_2Se_6])). A very short P–P bond length (206.7) which is even shorter than the P–P distance in the crystal structure of Ni_2[P_2Se_6] ([24]; 214.8 pm) is present in the crystal structure

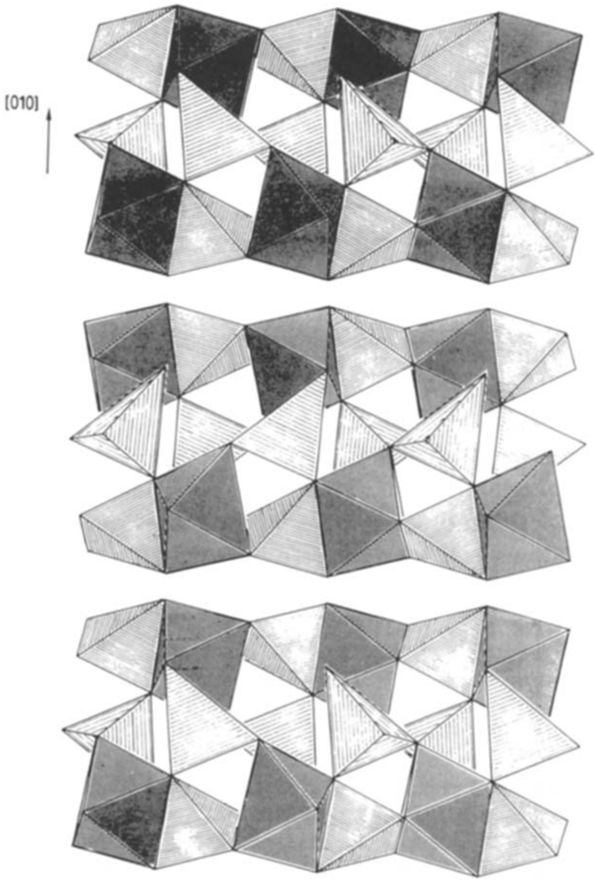

Fig. 7. Crystal structure of α-AgGa[P_2Se_6]; polyhedral representation. Selenium atoms occupy the apices of octahedra and tetrahedra. The octahedra contain the P_2 pairs, the darkly shaded tetrahedra contain Ga^{III} and the lightly shaded tetrahedra Ag^I.

of β-AgGa[P_2Se_6]; together with the comparatively long P–Se distance of 221.1 pm the bonding conditions underline the metastable character of this quaternary β-phase.

P–P and P–Se bond lengths (225.9 pm and 213.8–224.4 pm) in the crystal structure of α-AgGa[P_2Se_6] are of the same order as observed in the crystal structures of CuIn[P_2Se_6] and CuCr[P_2Se_6] and are also consistent with the respective values in the crystal structure of Ag_4[P_2Se_6] ([2]; 230 pm and 216–222 pm). Ga–Se distances (tetrahedral coordination of Ga^{III}; 239.6–245.6 pm) in the crystal structure of α-AgGa[P_2Se_6] are shorter than the Ga–Se bonds of Ga^{III} with octahedral coordination (262.6 pm in β-AgGa[P_2Se_6]); the Ag–Se bonds (Ag^I in tetrahedral coordination; 259.5–290.0 pm) in the crystal structure of α-AgGa[P_2Se_6] are of the same order as observed in the crystal structure of Ag_4[P_2Se_6] ([2]; 262.3–286.8 pm). As a common feature the [$AgSe_4$] tetrahedra in the crystal structures of the

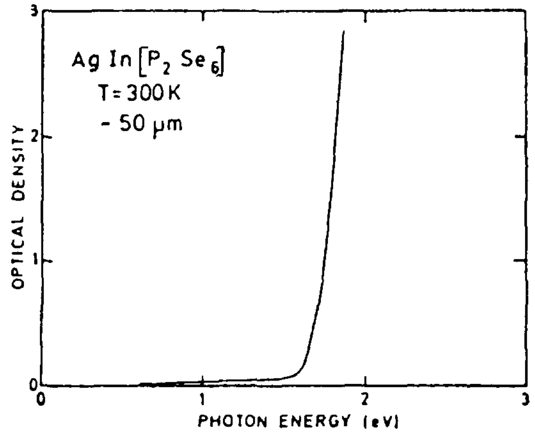

Fig. 8. Optical absorption of AgIn[P_2Se_6] at 300 K.

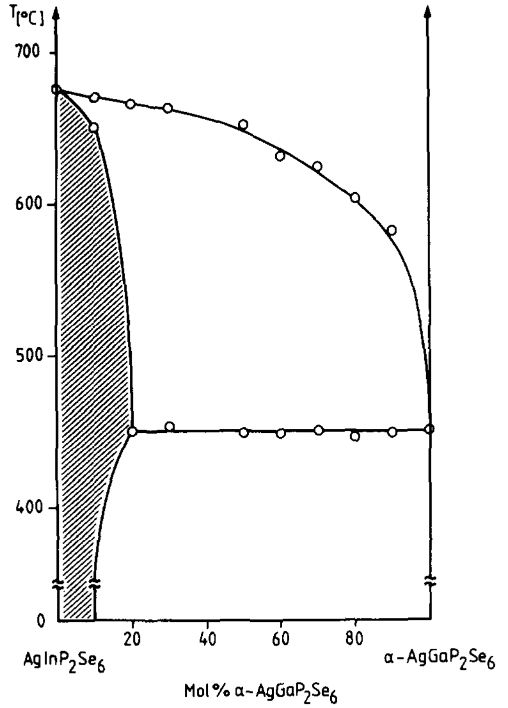

Fig. 9. Phase relations in the quasibinary system AgIn[P_2Se_6]/α-AgGa[P_2Se_6]. DTA investigation during heating (3 °C min^{-1}; Ni–NiCr; inert reference); the samples were quenched from the melt and annealed at 400 °C (21 d). Phase compositions at normal temperature were investigated by X-ray powder methods.

ternary and the quaternary phases are characterized by three shorter and one significantly longer Ag–Se distance.

From the viewpoint of application of the quaternary selenodiphosphates in the field of photovoltaic devices [9, 10], the most promising material between the compounds given in Table 1 seems to be the silver indium phase ($AgIn[P_2Se_6]$). The congruent melting behaviour together with the perfect layer structure (variant of the CdI_2-type structure) make it possible to grow thin films with crystallographic orientation directly from the melt. Thin layers of the material are of a dark red colour with a metallic lustre and show a sharp band-gap at $Eg = 1.79$ eV (Fig. 8). Variation of Eg should be realized by formation of solid solutions between isotypic phases (see Table 1) or at least by partial (limited) solid solutions, which is shown as an example in Fig. 9 for the quasibinary system between the non-isotypic phases $AgIn[P_2Se_6]$ and α-$AgGa[P_2Se_6]$. Further investigations in phase equilibria of multicomponent selenodiphosphate systems are in progress.

Acknowledgments

We thank Dr. K. Syassen, Dr. H. J. Beister and Mr. A. Breitschwerdt (Max-Planck-Institut für Festkörperforschung, Stuttgart) for optical absorption measurements and we also wish to acknowledge the support of this study by the Fonds der Chemischen Industrie and by the Freunde der TH-Darmstadt.

References

1 W. Klingen, G. Eulenberger and H. Hahn, *Z. Anorg. Allg. Chem.*, *401* (1973) 97.
2 P. Toffoli, P. Khodadad and N. Roier, *Acta Crystallogr.*, *Sect. B*, *34* (1978) 1779.
3 W. Welzel, *Ph.D. Thesis*, Universität Düsseldorf, 1987.
4 W. Klingen, R. Ott and H. Hahn, *Z. Anorg. Allg. Chem.*, *396* (1973) 271.
5 C. D. Carpentier and R. Nitsche, *Mater. Res. Bull.*, *9* (1974) 401.
6 M. Z. Jandali, G. Eulenberger and H. Hahn, *Z. Anorg. Allg. Chem.*, *447* (1978) 105.
7 A. Katty, S. Soled and A. Wold, *Mater. Res. Bull.*, *12* (1977) 663.
8 R. Diehl and C. D. Carpentier, *Acta Crystallogr.*, *Sect. B*, *34* (1978) 1097.
9 M. Etman, *Mater. Res. Bull.*, *17* (1982) 579.
10 T. Walter, R. Menner, L. Käser and H. W. Schock, Contributions to the *22nd IEEE Photovoltaic Specialists Conference*, 1991.
11 R. Pfeiff and R. Kniep, *GDCh Section of Solid State Chemistry*, 6th Conference Meeting, Siegen September 26–28, 1990.
12 Z. Ouili, A. Leblanc and P. Colombet, *J. Solid State Chem.*, *66* (1987) 86.
13 A. Leblanc, Z. Ouili and P. Colombet, *Mater. Res. Bull.*, *20* (1985) 947.
14 S. Lee, P. Colombet, G. Ouvrard and R. Brec, *Mater. Res. Bull.*, *21* (1986) 917.
15 P. Colombet, A. Leblanc, M. Danot and J. Rouxel, *J. Solid State Chem.*, *41* (1982) 174.
16 S. Lee, P. Colombet, G. Ouvrard and R. Brec, *Inorg. Chem.*, *27* (1988) 1291.
17 C. Payen, P. McMillan and P. Colombet, *Eur. J. Solid State Inorg. Chem.*, *27* (1990) 881.
18 G. Ouvrard and R. Brec, *Mater. Res. Bull.*, *23* (1988) 1199.
19 E. Durand, G. Ouvrard, M. Evian and R. Brec, *Inorg. Chem.*, *29* (1990) 4916.
20 H. M. Rietveld, *J. Appl. Cryst.*, *2* (1969) 65.
21 N. Walker and D. Stuart, *Acta Crystallogr.*, *Sect. A*, *39* (1983) 158.
22 G. M. Sheldrick, SHEXS 86, *An Integrated System for Solving, Refining and Displaying Crystal Structures from Diffraction Data*, University of Göttingen, 1986.
23 L. Pauling, *Die Natur der chemischen Bindung*, Chemie, Weinheim, 1962.
24 R. Brec, G. Ouvrard and J. Rouxel, *Mater. Res. Bull.*, *20* (1985) 1257.